Cycle Life Evaluation Based on Accelerated Aging Testing for Lithium-Ion Capacitors as Alternative to Rechargeable Batteries

Masatoshi Uno, *Member, IEEE*, and Akio Kukita

***Abstract*—Lithium-ion capacitors (LICs) are a hybrid energy storage device combining the energy storage mechanisms of lithium-ion batteries (LIBs) and electric double-layer capacitors (EDLCs), and are considered attractive not only in high-power applications but also as an alternative to rechargeable batteries due to their inherent long cycle life and relatively high energy density. The cycle life testing was performed for commercial-off-the-shelf LIC cells procured from three different manufactures, and the cycle life prediction model developed for EDLCs in the previous work was applied to LICs. Based on the resultant capacitance retention trends, the activation energies of degradation ratios were calculated using an Arrhenius equation, whereupon aging acceleration factors were determined. The calculated acceleration factors varied depending on manufacturers, suggesting that a proper aging acceleration factor should be determined for each manufacture cell based on cycle life testing rather than simply applying a rule of thumb which had been accepted for LIBs and EDLCs. The resulting and predicted capacitance retention trends correlated well, verifying that the cycle life prediction model established for EDLCs in the previous work would also be usable for LICs as an alternative to rechargeable batteries.**

***Index Terms* — Acceleration factor, aging, Arrhenius equation, cycle life prediction, lithium-ion capacitor (LIC), rechargeable battery**

I. Introduction

The use of rechargeable battery-based energy storage is increasingly expanding from portable electronic devices to large-scale systems, including electric vehicles and grid-connected applications. There are plenty of battery technologies available on the market, and, depending on applications, suitable battery technologies are selected considering their advantages and drawbacks.

Nowadays, the most prevalent rechargeable battery types are lead-acid, Ni-MH, and lithium-ion chemistries. The former technology prevails in industrial and telecommunication applications thanks to its technological maturity and cheap capital cost. However, their relatively low energy density characteristics and the periodic maintenance requirement limit their applications [1]. Ni-MH batteries are also a matured technology offering higher energy density while alleviating the need for periodic maintenance. Ni-MH batteries are not only used for portable electronic devices but also found in many hybrid electric vehicles [2], despite gradually being replaced by lithium-ion batteries (LIBs). LIBs are the optimal battery technology for portable electronic devices and electric vehicles because their energy density and specific energy are unrivaled among traditional rechargeable battery technologies [1], [2]. However, the risks of fire or, in the worst case, explosion due to overcharging, abuse, or mechanical damage are often cited as top concerns.

Conversely, supercapacitors, formally known as electric double-layer capacitors (EDLCs), are a form of energy storage that does not rely on chemical reaction for energy storage mechanisms, offering some remarkable major advantages over traditional rechargeable batteries, such as extended cycle life, higher power capability, improved safety, and extended allowable operational temperature range. However, since their specific energy (< 10 Wh/kg) is relatively lower than those of rechargeable batteries, EDLCs are mainly used in hybrid power systems [3]–[8], including regenerative systems [9] and electric vehicles [10]–[13], whereby EDLCs operate as high-power energy buffers to complement main rechargeable batteries. Dynamic behavior of EDLCs aiming at the adaptation to such hybrid applications have also been modeled [14], [15].

As a more viable candidate, lithium-ion capacitors (LICs) have been developed and commercialization attempts have already been made by several manufacturers. LICs are a hybrid energy storage device that combines the energy storage mechanisms of EDLCs and LIBs, realizing the advantages of EDLCs (i.e. the high power capability, extended cycle life, and widened operational temperature range) at a relatively high specific energy of > 14 Wh/kg [16]. Detailed characterization for LICs [16]–[18], comparison with traditional EDLCs [19]–[21], and modeling [22] have been performed, and, similar to conventional EDLCs, LICs are attracting significant attention, particularly in high-power applications such as a railway vehicle application [23]. Vigorous research and development efforts in search of better active materials targeting for such high-power applications are underway [24]–[27].

Manuscript received November 9, 2014; revised April 8, 2015 and July 23, 2015; accepted October 8, 2015.

Masatoshi Uno is with Ibaraki University, Ibaraki 316-8511, Japan (e-mail: masatoshi.uno.ee@vc.ibaraki.ac.jp).

Akio Kukita is with Japan Aerospace Exploration Agency, Kanagawa 252-5210, Japan (e-mail: kukita.akio@ jaxa.jp).

LICs represent a potential to be an alternative to traditional rechargeable batteries in various applications; from memory back-up and portable power supply to spacecraft power systems. For example, a feasibility study on spacecraft power systems using LICs suggests that a LIC-based power system would be a lighter power system with a longer cycle life than traditional LIB-based systems [28], driving expectations that LICs would be usable in not only hybrid energy storage systems but also many other applications. A small scientific spacecraft containing a technology demonstration platform to demonstrate long-term performance of a LIC under space environment was developed [29] and launched in September of 2013, and the LIC has been performing well as of this writing [30].

Since LICs are basically a long-life energy storage source, life testing under real time span and operation conditions is naturally impractical. In typical spacecraft applications, for example, life testing in a real time span for the typical cycle life requirement of 30,000 cycles takes approximately 5 years, compelling spacecraft designers to use obsolete devices that were developed more than 5 years ago. In addition, systems cannot be optimally designed without properly predicting cycle life performance of LICs under practical conditions. Therefore, not only is there a need for accelerated aging testing to cope with the sluggish life testing but also a proper cycle life prediction model is needed for designers to effectively design energy storage systems using LICs.

Life testing for LICs has been performed [24]–[27] but accelerated aging testing and cycle life prediction model for LICs have not been established yet. In addition, most previous works for cycle life testing involved laboratory cells, rather than commercial cells. To expedite penetration of LICs into industry and commercial applications, life testing using commercial-off-the-shelf (COTS) cells is considered indispensable. Furthermore, most previous life testing and characterization for LICs were performed focusing on high-power applications, and few research work has been carried out targeting for LICs as an alternative to rechargeable batteries.

On the other hand, calendar and cycle life performances of EDLCs have been characterized and evaluated by many researchers [31]–[36], and aging behaviors and degradation mechanisms have been addressed and discussed thoroughly [37]–[42]. Aging acceleration by elevating temperature and/or increasing applied voltage has been discussed [43]–[45], and the rule of thumb that degradation doubles for every 10°C increase or 100 mV increase is commonly accepted for EDLCs under floating conditions [46]–[48]. A cycle life prediction model for EDLCs as an alternative to rechargeable batteries has also been established based on accelerated charge-discharge cycling tests [49]. Aging of EDLCs can be accelerated by elevating temperature, and the aging acceleration factor was determined based on Arrhenius Law with degradation tendencies of EDLC cells cycled at three different temperatures. Meanwhile, the evolution of capacitance fade is nearly proportional to the square root of number of cycles and the derived cycle life prediction model satisfactorily matched experimental cycle life trends. Since LICs are a kind of supercapacitor, this cycle life prediction model established for EDLCs [49] could potentially be applied to LICs, facilitating the penetration of LICs in practical use.

The work of this paper is basically research extending the previous work performed for EDLCs [49]. LIC cells procured from three different manufacturers were cycled at various temperatures, and their cycle life trends were analyzed and modeled using the cycle life prediction model developed in the previous work [49]. The chief objectives of this study are to evaluate the cycle life of LIC cells as an alternative to rechargeable batteries and to investigate whether the cycle life prediction model developed for EDLCs [49] can be applied to LICs—investigating the degradation mechanism of LICs is outside the scope. To our knowledge, this is the first article reporting results of long-term cycle life testing, accelerated aging, and the cycle life prediction model for COTS LIC cells as an alternative to rechargeable batteries.

The rest of this paper is organized as follows. Experimental conditions, including specifications of COTS cells and cycling conditions, are explained in Section II and the results of charge-discharge cycling tests performed under various conditions are presented in Section III. Based on the degradation trends at different temperature conditions, aging acceleration factors are determined according to Arrhenius equation in Section IV. In Section V, it is verified that the cycle life prediction model established in the previous work is applicable to LICs, and the predicted cycle life performances of three different COTS cells are compared.

II. Experimental Conditions

A. Lithium-Ion Capacitor Cells

Both pouch- and can-type cells are available in the market. Pouch cells are considered preferable as an alternative to rechargeable batteries because of their higher specific energy and energy density than can-type cells. COTS pouch cells were procured from Manufacturers A–C (names not specified for contractual reasons) to evaluate the cycle life performance of LICs. The rated capacitances of these LIC cells were around 2500 F. Cells from each manufacturer were procured in different seasons, meaning the life testing for cells from each manufacturer were non-concurrent and the temperature conditions also differed slightly (see Table I). The numbers of

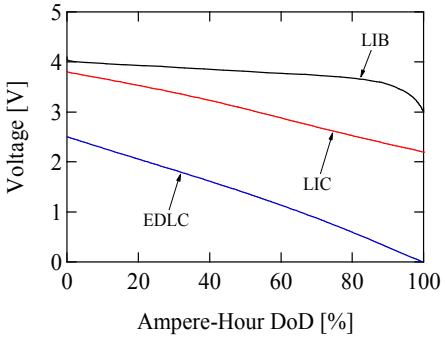

Fig. 1. Discharge curves of LIB, EDLC, and LIC cells.

cells assigned for life testing also differed for each manufacturer; nice cells for Manufacturer A, and fifteen cells for Manufacturers B and C—no cell from Manufacturer A was assigned for float conditions.

B. Depth of Discharge (DoD)

Discharge curves of a LIB, EDLC, and LIC are compared in Fig. 1. In practical use, the charging current and voltage for cells are regulated by a charger, while cells are discharged to loads via a dc–dc converter that behaves as a constant power (CP) load viewed from the cells. A constant-current (CC) discharging scheme is generally used in life testing for LIBs and is considered acceptable, even for CP loads, because of the relatively flat discharge curve, as shown in Fig. 1. Conversely, since the LIC voltage (as well as EDLC) varies significantly, a CP discharging scheme rather than simply using a CC discharging scheme is considered preferable for the life testing of LIC cells.

For cycle life testing of LIBs, the depth-of-discharge (DoD) is generally defined as the ratio of the discharged ampere-hour capacity to the rated capacity. This ampere-hour DoD, D_{Ah}, is convenient for cycle life testing of LIBs using the CC discharging scheme because the discharged capacity is invariably constant in every charge-discharge cycle. For the cycle life testing of LICs using the CP discharging scheme, on the other hand, the discharged ampere-hour capacity varies with voltage decline due to ageing, whereas the discharged energy is invariably constant in every cycle [49]. In other words, DoD for cycle life testing of LICs using the CP discharging scheme should be defined based on the discharged energy.

Similar to the cycle life testing performed for EDLCs in the previous work [49], DoD for LICs in this study is defined as the energy DoD, D_E, that is the ratio of discharged energy to rated stored energy. In general, the discharged capacity of capacitors, including LICs and EDLCs, is essentially equivalent to discharged charge, and therefore, D_{Ah} of capacitors is a function of voltage ($Q = CV$ where Q is the charge in coulomb and C is the capacitance in farad). On the other hand, the energy of capacitors is proportional to the square of voltage ($E = 0.5CV^2$ where E is the energy). According to [49], D_{Ah} and D_E are given by

$$D_{Ah} = \frac{CV_{cha} - CV_{EoD}}{CV_{cha} - CV_{cut-off}} = \frac{V_{cha} - V_{EoD}}{V_{cha} - V_{cut-off}}, \quad (1)$$

$$D_E = \frac{0.5CV_{cha}^{\ 2} - 0.5CV_{EoD}^{\ 2}}{0.5CV_{cha}^{\ 2} - 0.5CV_{cut-off}^{\ 2}} = \frac{V_{cha}^{\ 2} - V_{EoD}^{\ 2}}{V_{cha}^{\ 2} - V_{cut-off}^{\ 2}}, \quad (2)$$

where V_{cha} and $V_{cut\text{-}off}$ are the charge- and cut-off voltages, respectively, and V_{EoD} is the voltage at the end of discharge. From

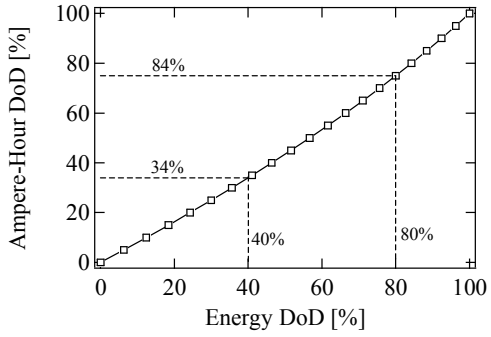

Fig. 2. Relationship between ampere-hour DoD (D_{Ah}) and energy DoD (D_E).

TABLE I. CHARGE-DISCHARGE CYCLING CONDITIONS.

Cell No.	Discharge (D_E)	Charge (V_{cha})	Temperature
1	80%	3.8 V	0°C
2	40%		
3		3.6 V	
4	No discharging	3.8 V (CV)	
5	(CV condition)	3.6 V (CV)	
6	80%	3.8 V	25°C (for Manufacture A) 30°C (for Manufacture B) 30°C (for Manufacture C)
7	40%		
8		3.6 V	
9	No discharging	3.8 V (CV)	
10	(CV condition)	3.6 V (CV)	
11	80%	3.8 V	40°C (for Manufacture A) 50°C (for Manufacture B) 60°C (for Manufacture C)
12	40%		
13		3.6 V	
14	No discharging	3.8 V (CV)	
15	(CV condition)	3.6 V (CV)	

*CV: Constant Voltage

(1) and (2), the relationship between D_E and D_{Ah} is yielded as

$$D_E = \frac{V_{cha}^{\ 2} - \left\{V_{cha} - D_{Ah}\left(V_{cha} - V_{cut-off}\right)\right\}^2}{V_{cha}^{\ 2} - V_{cut-off}^{\ 2}}. \quad (3)$$

The relationship between D_E and D_{Ah} of a LIC cell with a typical operational voltage range of 2.2–3.8 V is depicted in Fig. 2.

C. Cycling Conditions

LIC cells were cycled with constant-current–constant-voltage (CC–CV) charging and CP discharging schemes. A single charge-discharge cycle comprises 65-min CC–CV charging and 35-min CP discharging, emulating typical cycling condition for low-Earth-orbit spacecraft [50].

To investigate the degradation dependence on DoD, charge voltage, and temperature, cells were cycled at two DoDs, two charge voltages, and three temperatures, as shown in Table I, using the battery charge-discharge testing system (TOSCAT 3000, Toyo System). Three different temperatures in the test matrix were considered sufficient to determine the values of activation energy and aging acceleration factor as indispensable parameters for the cycle life prediction model, as will be discussed in detail in Section IV. In addition, floating tests (constant voltage) as reference test conditions were also performed for cells from Manufacturers B and C. All the current values in CC charging period were determined so that the CC and CV charging periods were 45 and 20 min, respectively, at the beginning of the cycle life

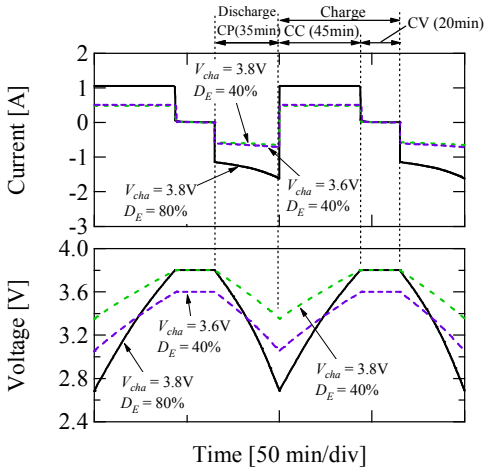

Fig. 3. Typical charge-discharge profiles during cycling.

testing. Typical charge-discharge cycling profiles (except for floating conditions) are shown in Fig. 3.

The capacitance retentions of LICs were periodically measured at 25°C in a thermostatic chamber. Cells were charged at a 1-C current rate of CC–CV (3.8 V) charging scheme for 5 hours and discharged at CC of 1-C rate until the cell voltages reached the lower limit of 2.2 V.

III. Experimental Results

As a representative capacitance measurement result, the discharge curve trend of Cell 11 from Manufacturer A is shown in Fig. 4. Inclinations of discharge curves gradually steepened and discharging time shortened with increasing number of cycles, indicating the gradual capacitance decay.

The capacitance retention trends of LIC cells from three manufacturers are shown in Fig. 5. Similar to traditional EDLCs as well as LIBs, the higher the temperature, the lower the capacitance retentions, suggesting that LIC aging can be accelerated by elevating temperature, as will be discussed in the next section. Conversely, the influence of cycling condition on the capacitance retention trends was insignificant (at least under the cycling condition used in our study), except for cells from Manufacturer B at D_E = 80% (i.e. Cells 1, 6, and 11.) The capacitance decays of these cells were obviously severer than the others, suggesting the DoD-dependent cycle life performance. On the other hand, cells from Manufacturers A and C under each temperature condition showed virtually uniform retention trends up until 10,000 and 5,000 cycles (approximately 700 and 350 days), respectively, and therefore, the life performance of these cells was DoD-independent, except for the deviant cell—Cell 11 from Manufacturer C is deemed to be possibly defective or having an unexpected detrimental event during testing because of the significant deviation from other trends and the sudden fall in capacitance retention, as shown in Fig. 5(c).

The resulting capacitance retention trends imply that the life performance of LICs might be influenced by cycling, depending on manufacturers. The cycle life performances of EDLCs are reportedly independent of cycle conditions [49], chiefly because EDLCs do not rely on chemical reactions for their energy storage mechanism. Conversely, some LIC cells showed DoD-dependent aging behaviors; capacitance retentions of cells from Manufacturer B cycled at D_E = 80% (i.e. Cells 1, 6 and 11) were explicitly lower than the others, as can be seen in Fig. 5(b). However, since cells cycled at D_E = 40% were seemingly unaffected up until 5,000 cycles, there could possibly be a threshold voltage and/or DoD condition that affects LICs' life performance.

The aging behaviors of LICs, shown in Fig. 5, varied depending on manufactures probably because of different materials used for each manufacture's cell, although materials used are not disclosed by manufactures. For example, a negative electrode, for which various carbon materials can be used, reportedly has significant influence on LIC performance [51]. Needless to say, other materials, such as electrolyte, carbon additive, binder, and positive electrode, are also considered to have substantial influence on cycle life performance. Thorough investigation based on electrochemical methodologies and more systematic and longer life testing would be indispensable to elucidate the underlying degradation mechanisms and detrimental cycling conditions, although this is outside the scope of this study.

It is noteworthy that cells tested under the float conditions

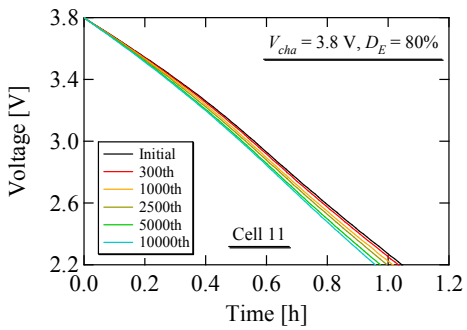

Fig. 4. Typical trend of discharge curves (e.g. Cell 11 from Manufacturer A).

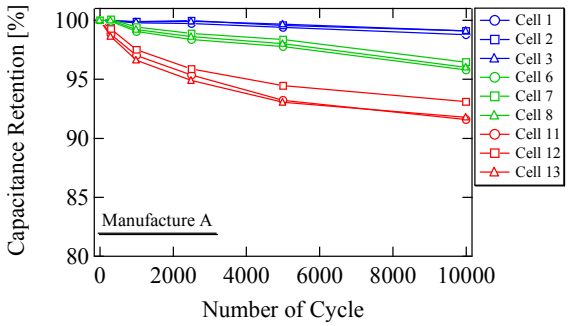

(a)

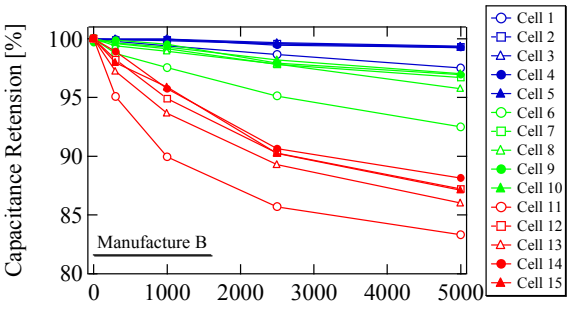

(b)

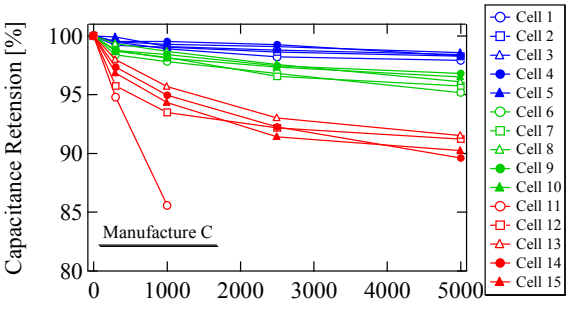

(c)

Fig. 5. Capacitance retention trends of LICs from Manufacturers (a) A, (b) B, and (c) C.

showed similar retention trends as those cycled, suggesting that float testing might be adequate and cycling might not necessarily be needed to evaluate LIC cells if used as an alternative to rechargeable batteries. In summary, except for the deep cycling condition of D_E = 80% for Manufacturer B cells, aging trends of LIC cells were insensitive to cycling conditions.

The previous work reported an empirical approach to predict aging trends of EDLCs [49]; degradation trends can be linearly extrapolated as a function of the square root of the number of cycles or testing time, as given by

$$C_T = 100 - D_T = 100 - d_T\sqrt{N}\,, \tag{4}$$

where C_T, D_T, and d_T are the capacitance retention, degradation ratio, and degradation rate constant at temperature T, respectively, and N is the number of cycles. The capacitance retention trends shown in Fig. 5 are redrawn in such a manner, as shown in Fig. 6. The resulting retention trends and extrapolated straight lines matched well, except for the deviant cell depicted as the dotted line in Fig. 6(c) (i.e. Cell 11 of Manufacturer C), suggesting that aging trends of LICs as an alternative to rechargeable batteries can be predicted similarly to [49].

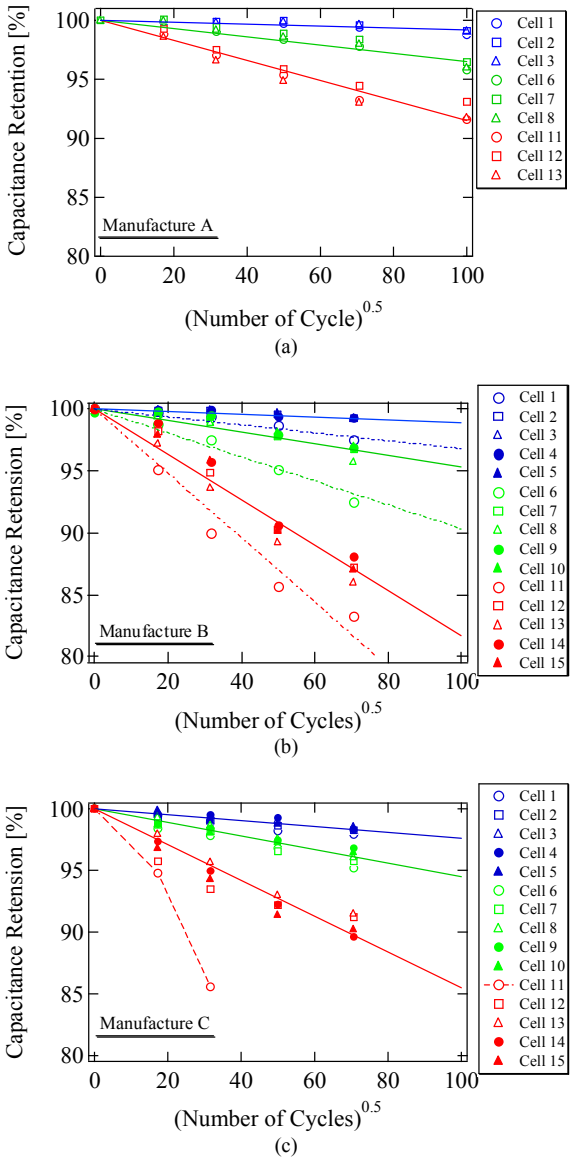

Fig. 6. Capacitance retention trends, as a function of square root of number of cycles, of LICs from Manufacturers (a) A, (b) B, and (c) C.

IV. Determination of Aging Acceleration Factor

A. Arrhenius Equation and Activation Energy

In the previous study for life testing for EDLCs [49], activation energies of degradation ratios are calculated based on the Arrhenius equation (see below) and used to determine the aging acceleration factor for degradation. In this section, according to the resulting capacitance retention trends shown in the previous section, the activation energies of degradation of cells from each manufacturer are obtained from the Arrhenius equation, followed by determination of acceleration factors.

The Arrhenius equation in the original form is given by

$$K = A\exp\left(\frac{-E_a}{RT}\right), \tag{5}$$

where K, A, E_a, R, and T are the rate of chemical reaction, coefficient, activation energy, gas constant, and temperature in Kelvin, respectively.

In general, high-surface area activated carbon is utilized as a positive electrode of LICs, similar to EDLCs, implying that the degradation mechanism of the positive electrode of LICs is similar to that of EDLCs, which has been reported in [37], [38]—the electrolyte and impurity are decomposed, and the decomposed product reduces accessibility of porous activated carbon electrodes, consequently reducing the effective capacitance. Meanwhile, a possible degradation mechanism of the negative electrode of LICs is also due to the decomposition of the electrolyte [52], [53]. The decomposition of the electrolyte and impurity is a kind of chemical side-reactions, suggesting that the Arrhenius equation can be applied to the degradation of LICs.

Assuming the degradation of LICs is due to chemical side-reactions, the degradation ratio at a given temperature, D_T, is considered proportional to K as $D_T \propto K$. By applying this relationship into (5), rearrangement form of (5) can be obtained as

$$\log D_T = \frac{1}{2.303}\frac{-E_a}{1000R}\frac{1000}{T} + \log A_D\,, \tag{6}$$

where $A_D \propto A$, and 1/2.303 is a conversion factor from natural to common logarithms. This equation indicates that if the degradation mechanism of LICs is governed by the Arrhenius equation and is homogeneous within a particular temperature range, the relationship between $\log D_T$ and $1000/T$ is characterized by a linear line with slope of $-E_a$. In general, $\log K (\propto \log D_T)$ graphed as a function of $1000/T$ is called an Arrhenius plot.

For the Arrhenius equation to be applied to determine the aging acceleration factor, the linearity of the Arrhenius plot in the tested temperature range needs to be confirm in the first place. A slope of a linear line in the Arrhenius plot is equal to the activation energy E_a (see (6)) that is the key parameter dictating the aging acceleration factor, as will be discussed in detail in Section IV-B. Nonlinearity of the Arrhenius plot implies not only that the degradation mechanism is not homogeneous in the tested temperature range but also that the aging acceleration factor is

temperature-dependent, making the aging acceleration infeasible. Hence, the Arrhenius equation should be applied in the proper temperature range that the linearity of the Arrhenius plot is confirmed from experimental results.

Arrhenius plots of the degradation trends of cells cycled at D_E = 80% from each manufacturer are shown in Fig. 7, as typical trends. The experimental results of degradation ratios at each cycle number were fitted to (6) using the least squares regression analysis. Except for data at $1000/T$ = 3.0 for the Manufacturer C cell (which was presumably defective as mentioned in the previous section), all the Arrhenius plots showed good linearity—even the Manufacture B cells cycled at D_E = 80% showed good linearity in the Arrhenius plot as shown in Fig. 7(b), although their capacitance retention trends were somewhat deviated from others (see Figs. 5(b) and 6(b)). These results imply that degradation of LIC cells is governed by the Arrhenius equation in the tested temperature range. Meanwhile, the degradation ratios of the Manufacture C cell cycled at D_E = 80% and 60°C (or at $1000/T$ = 3.0) did not obey the Arrhenius equation, suggesting that a different degradation mechanism might have taken place at this temperature or this cell was originally defective, as discussed in Section III-A.

In general, temperatures of cells under high-power cycling conditions are rather larger than ambient temperatures because of Joule heating in resistive components in cells [54], [55]. Conversely, if LICs are used as an alternative to rechargeable batteries, Joule heating is negligibly small because of low cycling currents and low resistance of LIC cells, and therefore, the degradation tendencies of LIC cells were considered well-governed by the Arrhenius equation. These results also suggest that aging acceleration is feasible by increasing temperature, as will be discussed in detail later.

The values of activation energies E_a of cells from each manufacture were also determined by applying the experimental results of degradation ratios into (6) using the least squares regression analysis—slopes of the fitting curves shown in Fig. 7

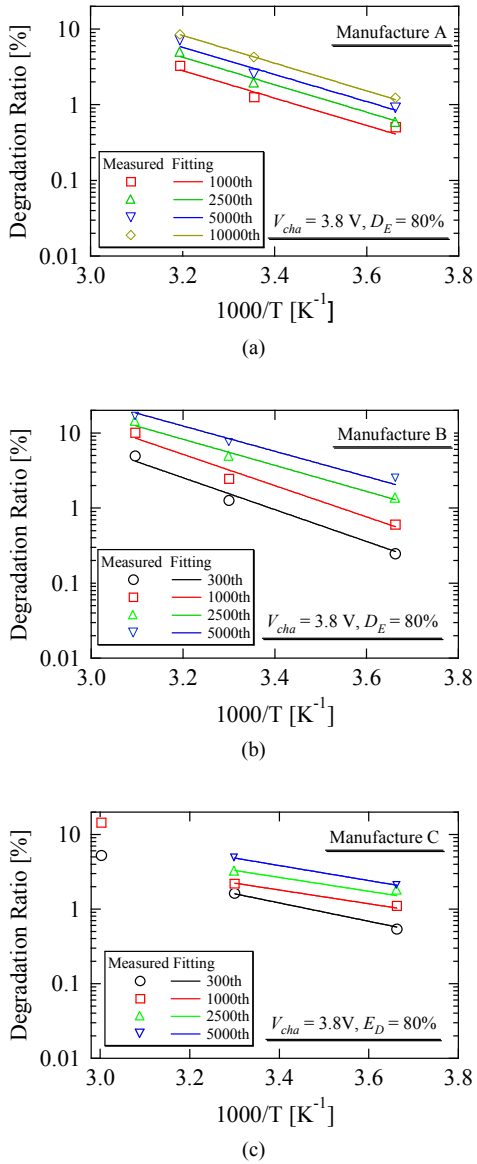

Fig. 7. Arrhenius plot trends of LICs from Manufacturers (a) A, (b) B, and (c) C.

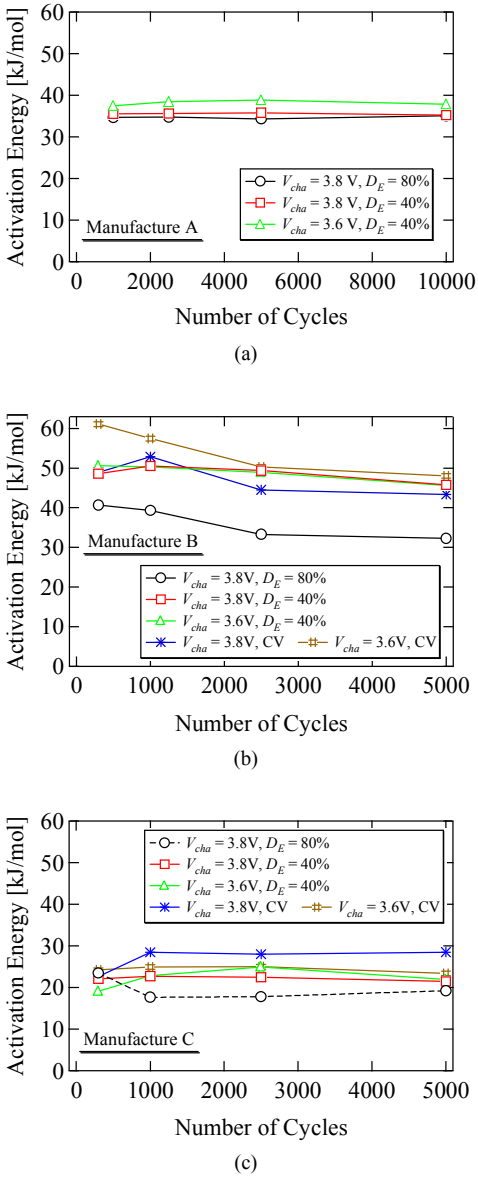

Fig. 8. Activation energy trends of LICs from Manufacturers (a) A, (b) B, and (c) C.

correspond to $-E_a$, as (6) indicates. The trends of E_a are shown in Fig. 8. The activation energy trends of cells from Manufacturers A and C were nearly independent of cycle conditions (except for the unreliable trend of Manufacturer C cells cycled at D_E = 80% because of the lack of data at 1000/T = 3.0, as aforementioned). Meanwhile, the trend of Manufacturer B cells at D_E = 80% was lower than the others. As discussed in the previous section, the capacitance retention trends of Manufacturer B cells at D_E = 80% were severer than the others and were seemingly affected by cycling. The different E_a trend not only reflects the deviated capacitance retention trends shown in Figs. 5(b) and 6(b) but also implies that the degradation mechanism of Manufacturer B cells at D_E = 80% was inhomogeneous to others cycled under different conditions because the different value of E_a for the same LIC cell indicates a different degradation reaction and/or mechanism taking place.

In summary, cells from each manufacturer showed different activation energy values. Aside from some deviant results originating from Manufacturers B and C cells cycled at D_E = 80%, the approximate values of E_a were 35, 48, and 21 kJ/mol for Manufacturers A, B, and C, respectively.

B. Aging Acceleration Factor

According to [46], the aging acceleration factor for every 10°C increase, α, is given by

$$\alpha = \sqrt[\left(\frac{T-T_{ref}}{10}\right)]{\frac{D_T}{D_{Tref}}} = \sqrt[\left(\frac{T-T_{ref}}{10}\right)]{\exp\left\{\frac{E_a}{R}\left(\frac{1}{T_{ref}}-\frac{1}{T}\right)\right\}}, \quad (7)$$

where D_{Tref} is the degradation ratio at the reference temperature of T_{ref}.

In general, α = 2, which indicates degradation doubles for every 10°C increase, is accepted for electrolytic capacitors, EDLCs [46]–[48], and LIBs. Based on the reported E_a values of 43–48 kJ/mol for LIBs [56], [57], α = 2 in the temperature range of 0–40° is considered reasonable for LIBs. In literature [46]–[48], α = 2 for EDLCs under float conditions was empirically confirmed. Conversely, in the previous study performed targeting for EDLCs as an alternative to rechargeable batteries, α = 1.2 is obtained based on the calculated E_a value of 13 kJ/mol [49].

Based on the approximate E_a values calculated in the previous subsection (35, 48, and 21 kJ/mol for Manufacturers A, B, and C, respectively), the aging acceleration factors were determined as α = 1.64, 2.26, and 1.45 in the tested temperature ranges. Accordingly, the determined α values vary depending on manufacturers, indicating that proper α values should be determined based on life testing rather than simply applying the widely-accepted rule of thumb of α = 2.

V. Cycle Life Prediction

A. Cycle Life Prediction Model

The previous study [49] derived the cycle life prediction model for EDLCs, as expressed below. Capacitance retention at a certain temperature and given cycle number can be predicted by

$$C_T = 100 - d_{Tref}\alpha^{\left(\frac{T-Tref}{10}\right)}\sqrt{N}, \quad (8)$$

where d_{Tref} is the degradation rate constant at temperature T_{ref}. Note that any tested temperatures can be chosen as T_{ref}, and d_{Tref} is determined from (4). This equation can be yielded by substituting (7) into (4). An estimated cycle life, N_{EoL}, can be yielded by rewriting (8), as

$$N_{EoL} = \left\{\frac{100 - C_{EoL}}{d_{Tref}\alpha^{\left(\frac{T-Tref}{10}\right)}}\right\}^2, \quad (9)$$

where C_{EoL} is the capacitance retention at the end of life that is usually defined as 80% of initial capacitance. The procedure of the cycle life prediction is summarized in Appendix.

B. Cycle Life Prediction for Tested LIC Cells

To apply the cycle life prediction model of (8), the values of d_{Tref} were determined using highest tested temperatures of 40, 50, and 60°C for cells from Manufacturers A, B, and C, respectively. The parameters used to predict cycle life are listed in Table II.

The predicted capacitance retention trends are shown in Fig. 9. Experimental capacitance retention trends, except for some deviant cell results, are also illustrated as reference data. Experimental and predicted capacitance retention trends matched satisfactorily, verifying that the cycle life prediction model of (8), which had been established for EDLCs, could also be applied to LICs as an alternative to rechargeable batteries.

Similar to the previous study [49], the highest possible operation temperatures for LICs to fulfill the spacecraft's typical cycle life requirement of 30,000 cycles were also determined using (8). The predicted capacitance retention trends at the highest possible operation temperatures are illustrated as solid lines in Fig. 9. Based on the predicted trends, temperatures of LICs from Manufacturers A, B, and C need to be maintained at least less than 45, 44.5, and 52.5°C, respectively, to meet the cycle life requirement of 30,000 cycles.

The values used in this study were determined and calculated using the experimental capacitance retention up until 10,000 or 5,000 cycles, which are equivalent to approximately 700 and 350 days, respectively. Parameters obtained from longer life testing and more data points would enable more accurate and reliable cycle life prediction.

Based on (9), the cycle lives of N_{EoL} for C_{EoL} = 80% as a function of temperature are predicted in the temperature range of 0–60°C, as shown in Fig. 10, in which a predicted cycle life of EDLCs [49] and experimentally-measured cycle lives of LIBs [58] are also shown as references—cycling conditions used in [49] and [58] are also to emulate low-Earth-orbit spacecraft conditions, similar to those in this study. Each LIC manufacturer showed different temperature-dependent cycle life trends. Manufacturer B cells were the most temperature-dependent, reflecting the highest value of E_a

TABLE II. PARAMETERS USED FOR CYCLE LIFE PREDICTIONS.

	Manufacture A	Manufacture B	Manufacture C
E_a	35 kJ/mol	48 kJ/mol	21 kJ/mol
R	8.314		
α	1.64	2.26	1.45
T_{ref}	40°C	50°C	60°C
d_{Tref}	0.09	0.18	0.15
C_{EoL}	80%		

(approximately 48 kJ/mol) among the three manufacturers. These temperature-dependent predicted cycle lives suggest that LIC cells should be properly chosen considering temperature dependency on life performance as well as the operational temperature ranges in target applications. Cells from Manufacturers B and C, for example, are expected to operate about 8×10^6 and 1×10^6 cycles at 10°C, respectively, whereas at the high temperature of 50°C, the predicted cycle lives are 1×10^4 and 4×10^4 cycles respectively. Based on the comparison of the three manufacturers from the cycle life perspective, cells from Manufacturer B are considered optimal for temperatures lower than approximately 37°C. For higher temperature applications, conversely, Manufacturer C cells would be advantageous in terms of cycle life. Needless to say, other important characteristics including specific energy, energy density, power capability, etc., should be taken into consideration to select the optimal for given applications.

In comparison with other energy storage sources from the cycle life point of view, LICs are greatly superior to LIBs, even though the LIBs were cycled at a shallow DoD (D_{Ah} = 20%)—in general, the shallower the DoD, the longer will be the cycle life of LIBs. Meanwhile, EDLCs are comparable to LICs, and its predicted cycle life is less temperature-dependent. From the comparison, in the temperature range lower than about 40°C, LICs offer longer cycle life performance than do EDLCs, suggesting that LICs can be a lighter energy storage source with longer service life than EDLCs. However, similar to the discussion above, proper comparisons in terms of not only the cycle life but also other factors, such as specific energy, cost, and technical maturity, need to be performed according to applications—for example, in [28], an LIC and LIB targeting for spacecraft power systems are compared from the view point of both cycle life and system weight.

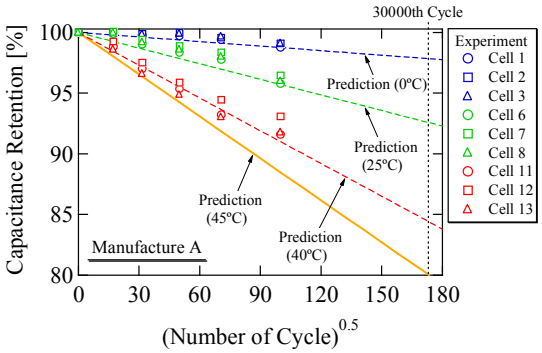

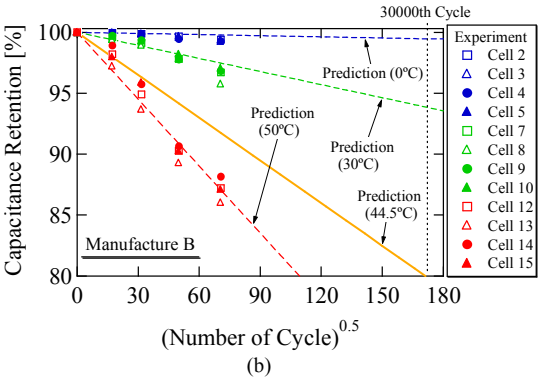

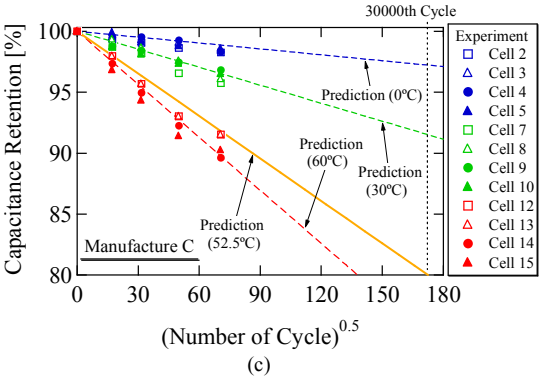

Fig. 9. Cycle life predictions for LICs from Manufacturers (a) A, (b) B, and (c) C.

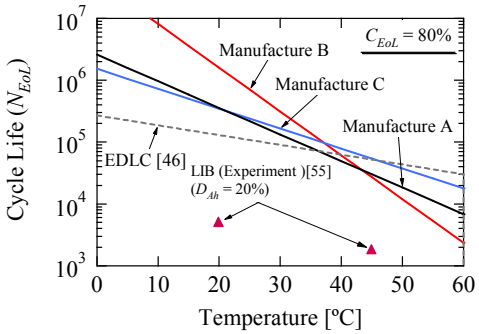

Fig. 10. Predicted cycle lives at given temperature.

VI. Conclusions

Cycle life performances of LIC cells as an alternative to rechargeable batteries were evaluated in this study. LIC cells were procured from three different manufacturers and were cycled at various DoDs, charge voltages, and temperatures for up to 10,000 cycles or approximately 700 days. The capacitance retention trends of LIC cells were chiefly dependent on temperatures; the higher the temperature, the more the LICs deteriorated, implying that aging can be accelerated by elevating temperatures.

The activation energy values of the degradation ratio of LIC cells were calculated using the Arrhenius equation, and were found to be nearly constant and independent of either cycle numbers, DoD, or charge voltage, except for some deviant cells. Based on the calculated activation energies, aging acceleration factors (α) were determined. The determined α values varied depending on manufacturers, suggesting that α should be determined from cycle life testing rather than simply applying the commonly-accepted rule of thumb of $\alpha = 2$, which had been used for traditional rechargeable batteries and EDLCs.

The cycle life prediction model established for EDLCs in the previous work was applied to LICs, with the determined α values. The experimental and predicted cycle life trends correlated effectively, verifying that the cycle lives of LICs as an alternative to rechargeable batteries could be predicted in a manner similar to EDLCs. α values determined from a longer cycle life testing and more data points would enable more accurate and reliable cycle life prediction.

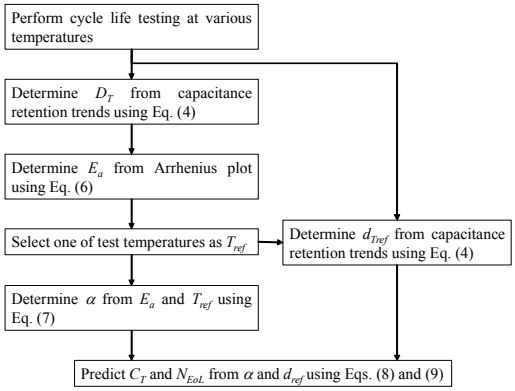

Fig. 11. Procedure of cycle life prediction.

VII. Appendix—Procedure of Cycle Life Prediction

In Fig. 11, the procedure of the cycle life prediction is summarized in the form of flowchart. First of all, cycle life testing is performed at various temperatures (at least two but desirably more than three temperatures). From the experimental results of capacitance retention trends, D_T and d_T are obtained from (4), followed by determination of E_a by substituting D_T into the Arrhenius equation (6) using the least squares regression analysis. To determine α, T_{ref} needs to be selected from test temperatures (e.g., one of 0°C, 25°C, and 40°C can be T_{ref} for Manufacture A cells as shown in Table I). Substitution of E_a and T_{ref} into (7) yields α. At the same time, the degradation rate constant at T_{ref}, d_{Tref}, can be determined from (4). Finally, C_T and N_{EoL} can be predicted by applying α and d_{Tref} into (8) and (9), respectively.

It is noteworthy that α slightly varies depending on which test temperature is applied to T_{ref} and T into (7), slightly influencing the predicted capacitance retention trends of C_T and N_{EoL}. It is advised that T_{ref} and T are selected so that experimental and predicted capacitance retention trends are in good agreement.

References

[1] E. M. Krieger, J. Cannarella, and C. B. Arnold, "A comparison of lead-acid and lithium-based battery behavior and capacity fade in off-grid renewable charging applications," *Energy*, vol. 60, pp. 492–500, Oct. 2013.

[2] J. Kang, F. Yan, P. Zhang, and C. Du, "Comparison of comprehensive properties of Ni-MH (nickel-metal hydride) and Li-ion (lithium-ion) batteries in terms of energy efficiency," *Energy*, vol. 70, pp. 618–625, Jun. 2014.

[3] U. K. Madawla, D. J. Thrimawithana, and N. Kularatna, "An ICPT-supercapacitor hybrid system for surge-free power transfer," *IEEE Trans. Ind. Electron.*, vol. 54, no. 6, pp. 3287–3297, Dec. 2007.

[4] P. Thounthong, S. Rael, and B. Davat, "Control strategy of fuel cell and supercapacitors association for a distributed generation system," *IEEE Trans. Ind. Electron.*, vol. 54, no. 6, pp. 3225–3233, Dec. 2007.

[5] C. Abbey and G. Joos, "Supercapacitor energy storage for wind energy applications," *IEEE Trans. Ind. Appl.*, vol. 43, no. 3, pp. 769–776, May–Jun. 2007.

[6] J. Jia, G. Wang, Y. T. Cham, Y. Wang, and M. Han, "Electrical characteristic study of a hybrid PEMFC and ultracapacitor system," *IEEE Trans. Ind. Electron.*, vol. 57, no. 6, pp. 1945–1953, Jun. 2010.

[7] W. Li, G. Joós, and J. Bélanger, "Real-time simulation of a wind turbine generator coupled with a battery supercapacitor energy storage system," *IEEE Trans. Ind. Electron.*, vol. 57, no. 4, pp. 1137–1145, Apr. 2010.

[8] S. Lemofouet and A. Rufer, "A hybrid energy storage system based on compressed air and supercapacitors with maximum efficiency point tracking (MEPT)," *IEEE Trans. Ind. Electron.*, vol. 53, no. 4, pp. 1105–1115, Jun. 2006.

[9] P. J. Grbovic, P. Delarue, P. L. Moigne, and P. Bartholomeus, "Modeling and control of the ultracapacitor-based regenerative controlled electric drives," *IEEE Trans. Ind. Electron.*, vol. 58, no. 8, pp. 3471–3484, Aug. 2011.

[10] M. Ortuzar, J. Moreno, and J. Dixon, "Ultracapacitor-based auxiliary energy system for an electric vehicle: implementation and evaluation," *IEEE Trans. Ind. Electron.*, vol. 54, no. 4, pp. 2147–2156, Aug. 2007.

[11] Y. Hyunjae, S. K. Sul, Y. Park, and J. Jongchan, "System integration and power-flow management for a series hybrid electric vehicle using supercapacitors and batteries," *IEEE Trans. Ind. Appl.*, vol. 44, no. 1, pp. 108–114, Jan.–Feb. 2008.

[12] J. Moreno, M. E. Ortúzar, and J. W. Dixon, "Energy-management system for a hybrid electric vehicle, using ultracapacitors and neural networks," *IEEE Trans. Ind. Electron.*, vol. 53, no. 2, pp. 614–623, Apr. 2006.

[13] A. L. Allègre, A. Bouscayrol, P. Delarue, P. Barrade, E. Chattot, and S. E. Fassi, "Energy storage system with supercapacitor for an innovative subway," *IEEE Trans. Ind. Electron.*, vol. 57, no. 12, pp. 4001–4012, Dec. 2010.

[14] N. Bertrand, J. Sabatier, O. Brait, and J. M. Vinassa, "Embedded fractional nonlinear supercapacitor model and its parametric estimation method," *IEEE Trans. Ind. Electron.*, vol. 57, no. 12, pp. 3991–4000, Dec. 2010.

[15] V. Musolino, L. Piegari, and E. Tironi, "New full-frequency-range supercapacitor model with easy identification procedure," *IEEE Trans. Ind. Electron.*, vol. 60, no. 1, pp. 112–120, Jan. 2013.

[16] N. Omar, M. Daowd, O. Hegazy, M. A. Sakka, T. Choosemans, P. V. D. Bossche, and J. V. Mierlo, "Assessment of lithium-ion capacitor for using in battery electric vehicle and hybrid electric vehicle applications," *Electrochemica Acta*, vol. 86, pp. 305–315, Dec. 2012.

[17] N. Omar, M. A. Sakka, J. V. Mierlo, P. V. Bossche, and H. Gualous, "Electric and thermal characterization of advanced hybrid Li-ion capacitor rechargeable energy storage system," in Proc. *Power Eng. Energy Electrical Drives (POWERENG)*, pp. 1574–1580, May 2013.

[18] N. Omar, J. Ronsmans, Y. Firozu, M. A. Monem, A. Samba, H. Gualous, O. Hegazy, J. Smekens, T. Coosemans, P. V. Bossche, and J. V. Mierlo, "Lithium-ion capacitor—Advanced technology for rechargeable energy storage systems," in Proc. *Electric Veh. Sympo. Exhibition (EVS27)*, pp. 1–11, Nov. 2013.

[19] V. Musolino and E. Tironi, "A comparison of supercapacitor and high-power lithium batteries," in Proc. *Electrical Systems for Aircraft, Railway and Ship Propulsion (ESARS)*, pp. 1–6, Oct. 2010.

[20] S. M. Lambert, V. Pickert, J. Holden, X. He and W. Li, "Comparison of supercapacitor and lithium-ion capacitor technologies for power electronics applications," in Proc. *Power and Electron. Machines and Drives*, pp. 19–21, Apr. 2010.

[21] R. B. Sepe, A. Steyerl, and S. P. Bastien, "Lithium-ion supercapacitors for pulse power applications," in Proc. *IEEE Energy Conversion Congress and Exposition (ECCE)*, pp. 1813-1818, Sep. 2011.

[22] S. Barcellona, F. Ciccarelli, D. Iannuzzi, and L. Piegari, "Modeling and parameter identification of lithium-ion capacitor modules," *IEEE Trans. Sustainable Energy*, vol. 5, no. 3, pp. 785–794, Jul. 2014.

[23] F. Ciccarelli, A. D. Pizzo, and D. Iannuzzi, "Improvement of energy efficiency in light railway vehicles based on power management control of wayside lithium-ion capacitor storage," *IEEE Trans. Power Electron.*, vol. 29, no. 1, pp. 275–286, Jan. 2014.

[24] N. Böckenfeld, R. S. Kühnel, S. Passerini, M. Winter, and A. Balducci, "Composite $LiFePO_4$/AC high rate performance electrodes for Li-ion capacitors," *J. Power Sources*, vol. 196, no. 8, pp. 4136–4142, Apr. 2011.

[25] H. Konno, T. Kasashima, and K. Azumi, "Application of Si-C-O glass-like compounds as negative electrode materials for lithium hybrid capacitors," *J. Power Sources*, vol. 191, no. 15, pp. 623–627, Jun. 2009.

[26] X. Sun, X. Zhang, H. Zhang, N. Xu, K. Wang, and Y. Ma, "High performance lithium-ion hybrid capacitors with pre-lithiated hard carbon anodes and bifunctional cathode electrodes," *J. Power Sources*, vol. 270, pp. 318–325, Dec. 2014.

[27] A. Brandt and A. Balducci, "A study about the use of carbon coated iron oxide-based electrodes in lithium-ion capacitors," *Electrochemica Acta*, vol. 108, pp. 219–225, Oct. 2013.

[28] M. Uno and K. Tanaka, "Spacecraft electrical power system using lithium-ion capacitors," *IEEE Trans. Aerosp. Electron. Syst.*, vol. 49, no. 1, pp. 175–188, Jan. 2013.

[29] A. Kukita, M. Takahashi, K. Shimazaki, H. Toyota, M. Imaizumi, Y. Kobayashi, T. Takamoto, M. Uno, and T. Shimada, "On-orbit

demonstration of thin-film multi-junction solar cells and lithium-ion capacitors as bus components," in Proc. *9th European Space Power Conf. (ESPC)*, Jun. 2011.
[30] A. Kukita, M. Takahashi, K. Shimazaki, Y. Kobayashi, T. Sakai, H. Toyota, Y. Takahashi, M. Murashima, M. Uno, and M. Imaizumi, "On-orbit demonstration of a lithium-ion capacitor and thin-film multijunction solar cells," in Proc. *10th European Space Power Conf. (ESPC)*, Apr. 2014.
[31] N. Rizoug, P. Bartholomeus, and P. L. Moigne, "Modeling and characterizing supercapacitors using an online method," *IEEE Trans. Ind. Electron.*, vol. 57, no. 12, pp. 3980–3990, Dec. 2010.
[32] A. Hammar, P. Venet, R. Lallemand, G. Coquery, and G. Rojat, "Study of accelerated aging of supercapacitors for transport applications," *IEEE Trans. Ind. Electron.*, vol. 57, no. 12, pp. 3972–3973, Dec. 2010.
[33] H. Gualous, R. Gallay, M. A. Sakka, A. Oukaour, B. T. Ighil, and B. Boudart, "Calendar and cycling ageing of activated carbon supercapacitor for automotive application," *Microelectronics Reliability*, vol. 52, no. 9–10 pp. 2477–2481, Sep.–Oct. 2012.
[34] A. Oukaour, B. T. Ighil, M. A. Sakka, H. Gaulous, R. Gallay, and B. Boudart, "Calender ageing and health diagnosis of supercapacitor," *Electric Power Systems Research*, vol. 95, pp. 330–338, Feb. 2013.
[35] M. Ristic, Y. Gryska, J.V.M. McGinley, and V. Yufit, "Supercapacitor energy storage for magnetic resonance imaging systems," *IEEE Trans. Ind. Electron.*, vol. 61, no. 8, pp. 4255–4264, Aug. 2014.
[36] P. Kreczanik, P. Venet, A. Hijazi, and G. Clerc, "Study of supercapacitor aging and lifetime estimation according to voltage, temperature, and RMS current," *IEEE Trans. Ind. Electron.*, vol. 61, no. 9, pp. 4895–4902, Sep. 2014.
[37] E. H. E. Brouji, O. Briat, J. M. Vinassa, N. Bertrand, and E. Woirgard, "Impact of calendar life and cycling ageing on supercapacitor performance," *IEEE Trans. Veh. Technol.*, vol. 58, no. 8, pp. 3917–3929, Oct. 2009.
[38] O. Briat, J. M. Vinassa, N. Bertrand, H. E. Brouji, J. Y. Deletage, and E. Woirgard, "Contribution of calendar ageing modes in the performances degradation of supercapacitors during power cycling," *Microelectronics Reliability*, vol. 50, no. 9–11, pp. 1796–1803, Sep.–Nov. 2010.
[39] H. E. Brouji, O. Briat, J. M. Vinassa, N. Bertrand, and E. Woirgard, "Comparison between chang s es of ultracapacitors model parameters during calendar life and power cycling ageing tests," *Microelectronics Reliability*, vol. 48, no. 8–9, pp. 1473–1478, Aug.–Sep. 2008.
[40] R. Nozu, M. iizuka, M. Nakanishi, and M. Kotani, "Investigation of the life process of the electric double layer capacitor during float charging," *J. Power Sources*, vol. 186, no. 2, pp. 570–579, Jan. 2009.
[41] P. Azais, L. Duclaux, P. Florian, D. massiot, M. A. L. Rodenas, A. L. Solano, J. P. Peres, C. Jehoulet, and F. Beguin, "Causes of supercapacitors ageing in organic electrolyte," *J. Power Sources*, vol. 171, no. 2, pp. 1046–1053, Sep. 2007.
[42] M. Hahn, R. Kotz, R. Gallay, and A. Siggel, "Pressure evolution in propylene carbonate based electrochemical double layer capacitors," *Electrochemia Acta*, vol. 52, no. 4, pp. 1709–1712, Dec. 2006.
[43] H. Gualous, R. Gallay, G. Alcicek, B. T. Ighil, A. Oukaour, B. Boudart, and Ph. Makany, "Supercapacitor ageing at constant temperature and constant voltage and thermal shock," *Microelectronics Reliability*, vol. 50, no. 9–11, pp. 1783–1788, Sep.–Nov. 2010.
[44] T. Umemura, Y. Mizutani, T. Okamoto, T. Taguchi, K. Nakajima, and K. Tanaka, "Life expectancy and degradation behavior of electric double layer capacitor Part I," in Proc. *7th Int. Conf. Properties and Appl. of Dielectric Materials*, pp. 944–948, Jun. 2003.
[45] E. Schaeffer, F. Auger, Z. Shi, and P. Guillemet, "Comparative analysis of some parametric model structures dedicated to EDLC diagnosis," *IEEE Trans. Ind. Electron.*, to be published.
[46] P. Kurzwell and B. Frenzel, "Capacitance characterization methods and ageing behavior of supercapacitors," in Proc. *15th Int. seminar on Double Layer Capacitors*, pp. 1–12, Dec. 2005.
[47] R. Kotz, M. Hahn, and R. Gallay, "Temperature behavior and impedance fundamentals of supercapacitors," *J. Power Sources*, vol. 154, no. 2, pp. 550–555, Mar. 2006.
[48] O. Bohlen, J. Kowal, and D. U. Sauer, "Temperature behavior and impedance fundamentals of supercapacitors," *J. Power Sources*, vol. 172, no. 1, pp. 468–475, Oct. 2007.
[49] M. Uno and K. Tanaka, "Accelerated charge-discharge cycling test and cycle life prediction model for supercapacitors in alternative battery applications," *IEEE Trans. Ind. Electron.*, vol. 61, no. 9, pp. 3920–3930, Nov. 2012.
[50] M. Uno, K. Ogawa, Y. Takeda, Y. Sone, K. Tanaka, M. Mita, and H. Saito, "Development and on-orbit operation of lithium-ion pouch battery for small scientific satellite "REIMEI"," *J. Power Sources*, vol. 196, no. 20, pp. 8755–8763, Oct. 2011.
[51] J. H. Kim, J. S. Kim, Y. G. Lim, J. G. Lee, and Y. J. Kim, "Effect of carbon types on the electrochemical properties of negative electrodes," *J. Power Sources*, vol. 196, no. 23, pp. 10490–10495, Dec. 2011.
[52] C. Decaux, G. Lota, E. R. Pinero, E. Frackowiak and F. Beguin, "Electrochemical performance of a hybrid lithium-ion capacitor with a graphite anode preloaded from lithium bis (trifluoromethane) sulfonimide-based electrolyte," *Electrochemica Acta*, vol. 86, pp. 282–286, Dec. 2012.
[53] S. R. Sivakkumar and A. G. Pandolfo, "Evaluation of lithium-ion capacitors assembled with pre-lithiated graphite anode and activated carbon cathode," *Electrochemica Acta*, vol. 65, pp. 280–287, Mar. 2012.
[54] J. Schiffer, D. Linzen, and D. U. Sauer, "Heat generation in double layer capacitors," *J. Power Sources*, vol. 160, no. 1, pp. 765–772, Sep. 2006.
[55] K. Paul, M. Christian, V. Pascal, C. Guy, R. Gerard, and Z. Younes, "Constant power cycling for accelerated ageing of supercapacitors," in Proc. *European Conf. on Power Electron. Appl.*, pp. 1–10, Sep. 2009.
[56] H. Yoshida, N. Imamura, T, Inoue, K. Takeda, and H. Naito, "Verification of life estimation model for space lithium-ion cells," *Electrochemistry*, vol. 78, no. 5, pp. 482–488, 2010.
[57] Y. Mita, S. Seki, N. Terada, N. Kihira, K. Takei and H. Miyashiro, "Accelerated test methods for life estimation of high-power lithium-ion batteries," *Electrochemistry*, vol. 78, no. 5, pp. 382–386, 2010.
[58] S. Brown, K. Ogawa, Y. Kumeuchi, S. Enomoto, M. Uno, H. Saito, Y. Sone, D. Abraham, and G. Lindberg, "Cycle life evaluation of 3 Ah $Li_xMn_2O_4$-based lithium-ion secondary cells for low-earth-orbit satellites," *J. Power Sources*, vol. 195, no. 2, pp. 1444–1453, Dec. 2008.

Masatoshi Uno (M'06) was born in Japan in 1979. He received the B.E. degree in electronics engineering and the M.E. degree in electrical engineering from Doshisha University, Kyoto, Japan, in 2002 and 2004, respectively, and the Ph.D degree from the Graduate University for Advanced Studies, Kanagawa, Japan, in 2012.

In 2004, he joined Japan Aerospace Exploration Agency, Kanagawa, Japan, developing spacecraft power systems including battery, photovoltaic, and fuel cell systems. In 2014, he joined the Department of Electrical and Electronics Engineering, Ibaraki University, Ibaraki, Japan, where he is currently an Associate Professor of Electrical Engineering. His research interests include switching power converters, cell equalizers, life evaluation for supercapacitors and lithium-ion batteries, and development of fuel cell systems.

M. Uno is a member of the Institute of Electrical Engineering of Japan (IEEJ) and the Institute of Electronics, Information and Communication Engineers (IEICE).

Akio Kukita was born in Japan in 1967. He received the B.E. degree in physics from Chuo University, Japan, in 1993. From 1993 to 1996 and 1996 to 2008, he was with SEIKO Holdings Corporation and Ebara Corporation, respectively. Since 2008, he has been with Japan Aerospace Exploration Agency as a senior engineer. His recent work has focused on the development of spacecraft power systems.